Pergamon

SCIENCE DIRECT®

Tetrahedron 59 (2003) 10373–10380

TETRAHEDRON

Substituents effect on molecular structures of 13-vertex *closo*-metallacarboranes of rare earths. Synthesis and structural characterization of metallacarboranes bearing *nido*- and *arachno*-carborane ligands

Shaowu Wang,[a,b] Yaorong Wang,[a] Mak-Shuen Cheung,[a] Hoi-Shan Chan[a] and Zuowei Xie[a,*]

[a]*Department of Chemistry, The Chinese University of Hong Kong, Shatin, New Territories, Hong Kong, China*
[b]*Institute of Organic Chemistry, School of Chemistry and Materials Science, Anhui Normal University, Wuhu, Anhui 241000, China*

Received 12 April 2003; accepted 11 June 2003

Abstract—Several new 13-vertex *closo*-metallacarboranes of rare earths incorporating *nido*- and *arachno*-carborane ligands have been prepared and structurally characterized. They represent a new class of metallacarboranes bearing a η^7-carboranyl ligand recently discovered in our laboratory. This work indicates that the substituents on carborane cage carbons may affect the overall molecular structures of the resultant 13-vertex *closo*-metallacarborane complexes, but have little influence on the interactions between the central metal ion and *nido*- or *arachno*-carborane ligand.

1. Introduction

It has been documented that *o*-$C_2B_{10}H_{12}$ can be readily reduced by alkali metals to give the dianionic species [*nido*-$C_2B_{10}H_{12}]^{2-}$ which is a very useful synthon for the production of numerous metallacarboranes of s-, p-, d-, and f-elements.[1–3] Although *o*-carborane cannot be directly reduced to the *arachno* species, we have discovered that in the presence of f-block lanthanide metal halides, *o*-carborane can undergo four-electron reduction with excess alkali metals to form a *arachno*-$C_2B_{10}H_{12}^{4-}$ tetraanion that is capable of being η^7-bound to metal ions, leading to a new class of 13-vertex *closo*-metallacarboranes.[4–6]

Transition metal ions have a large influence on the formation of *arachno*-carborane tetraanions. Those with d^0/f^n electronic configuration are essential to stabilize the η^7-$C_2B_{10}H_{12}^{4-}$ anion, which is supported by DFT calculations.[6] On the other hand, effects of cage substituents on the formation of this class of 13-vertex *closo*-metallacarboranes and their molecular structures are largely unexplored. With this in mind, we have extended our research to mono- and bis-substituted *o*-carboranes. This paper reports the synthesis and molecular structures of several new 13-vertex *closo*-metallacarboranes of rare earths as well as substituents effect on the resultant metal complexes.

2. Results and discussion

2.1. Metallacarboranes with mono-substituted carborane ligands

2.1.1. Synthesis. Indenyl is a less electron rich, more sterically demanding yet planar π ligand than cyclopentadienyl. The former has demonstrated diverse bonding models (η^5–η^3–η^1) upon binding to transition metal ions,[7] which may influence the interactions between the central metal ion and carborane ligand. Reaction of $Me_2Si(C_9H_7)(C_2B_{10}H_{11})$ (**1**)[8] with excess NaH followed by treatment with excess Na metal presumably afforded the sodium salt of trianion, $\{Me_2Si(C_9H_6)(C_2B_{10}H_{11})\}\{Na_3(THF)_n\}$. Interaction of this salt with 1 equiv. of $ErCl_3$ in THF gave, after recrystallization from toluene/THF, $[\{\eta^5{:}\eta^6\text{-}Me_2Si(C_9H_6)(C_2B_{10}H_{11})\}Er(THF)(\mu\text{-}Cl)Na(THF)_2]_n$ (**2**) in 67% isolated yield. The *nido*-carborane in **2** accepted two more electrons from sodium to become the *arachno* species resulting in the isolation of $[\{\eta^5{:}\eta^7\text{-}[Me_2Si(C_9H_6)(C_2B_{10}H_{11})]Er\}_2\{Na_4(THF)_8\}]_n$ (**3**). This result was also achieved by 'one-pot' synthesis. Treatment of **1** with excess NaH in THF followed by reaction with $DyCl_3$ in the presence of excess Na produced, after work-up, $[\{\eta^5{:}\eta^7\text{-}[Me_2Si(C_9H_6)(C_2B_{10}H_{11})]Dy\}_2\{Na_4(THF)_8\}]_n$ (**4**),

Keywords: boron; carborane; cluster; lanthanide; metallacarborane; rare earth.
* Corresponding author. Tel.: +852-2609-6269; fax: +852-2603-5057; e-mail: zxie@cuhk.edu.hk

0040–4020/$ - see front matter © 2003 Elsevier Ltd. All rights reserved.
doi:10.1016/j.tet.2003.06.002

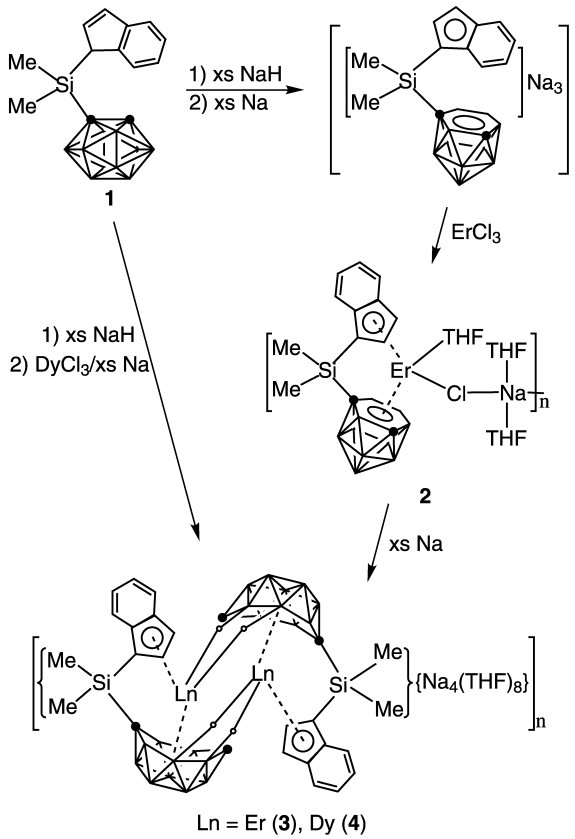

Scheme 1.

an analogue of **3**. These synthetic routes are outlined in Scheme 1.

Complexes **2**–**4** are extremely air- and moisture-sensitive but remain stable for months at room temperature under an inert atmosphere. They are soluble in polar organic solvents such as THF, DME, and pyridine, sparingly soluble in toluene, and insoluble in *n*-hexane. Both **3** and **4** decompose in CH_2Cl_2.

The NMR characterization of these complexes was precluded from paramagnetic property of Er^{3+} and Dy^{3+} ions. The indenyl–carboranyl ligand to THF ratios in **2**–**4** were measured by the ^1H NMR spectra of their hydrolysis products. It was necessary to perform single-crystal X-ray analyses in order to elucidate the metal–ligand bonding.

2.1.2. Molecular structure. The solid-state structure of **2** is shown in Figure 1. The Er^{3+} ion is η^5-bound to the five-membered ring of the indenyl group, η^6-bound to the hexagonal C_2B_4 face of the *nido*-carborane cage, σ-bound to one bridging chlorine atom and coordinated to one THF molecule in a distorted-tetrahedral arrangement. The associated complex cation $Na(THF)_2^+$ serves as a linkage to connect two $[\{\eta^5{:}\eta^6\text{-}Me_2Si(C_9H_6)(C_2B_{10}H_{11})\}Er(THF)(\mu\text{-}Cl)]^-$ fragments together, resulting in the formation of one-dimensional coordination polymeric chain (Fig. 2). It is noteworthy that the NaCl in **2** cannot be removed via recrystallization, which suggests high Lewis acidity of central metal ion caused by relatively poor electron-donating ability of the indenyl group. This result can be compared with the monomeric structure of $[\eta^5{:}\eta^6\text{-}Me_2C(C_5H_4)(C_2B_{10}H_{11})]Er(THF)_2$.[9] The Er–C($C_5$ ring) distances range from 2.588(13) to 2.787(15) Å with an average value of 2.675(15) Å (Table 1), indicating a slip distortion of Er toward the side of C(11)–C(12) bond. This measured value along with the average Er–C(cage) and Er–B(cage) distances of 2.740(12) and 2.790(16) Å are longer than the corresponding values found in its cyclopentadienyl analogue of $[\eta^5{:}\eta^6\text{-}Me_2C(C_5H_4)(C_2B_{10}H_{11})]Er(THF)_2$.[9] The Er–Cl(μ) distance of 2.563(4) Å and Na···Cl(μ) distance of 2.781(6) Å are all longer than the corresponding values of 2.545(1) and 2.633(2) Å found in $[\{\eta^5{:}\sigma\text{-}Me_2Si(C_9H_6)(C_2B_{10}H_{10})\}\{\eta^5\text{-}Me_2Si(C_9H_6)(C_2B_{10}H_{11})\}]Er(\mu\text{-}Cl)Na(THF)_3$, respectively.[10] Here, the Na···Cl(μ) is best described as an ionic interaction.

X-ray analyses reveal that complexes **3** and **4** are isostructural and isomorphous. Figure 3 shows their representative structure, clearly indicating the presence of the *arachno*-carborane. They are coordination polymers. Each asymmetrical unit contains two identical $\{[\eta^5{:}\eta^7\text{-}Me_2Si$

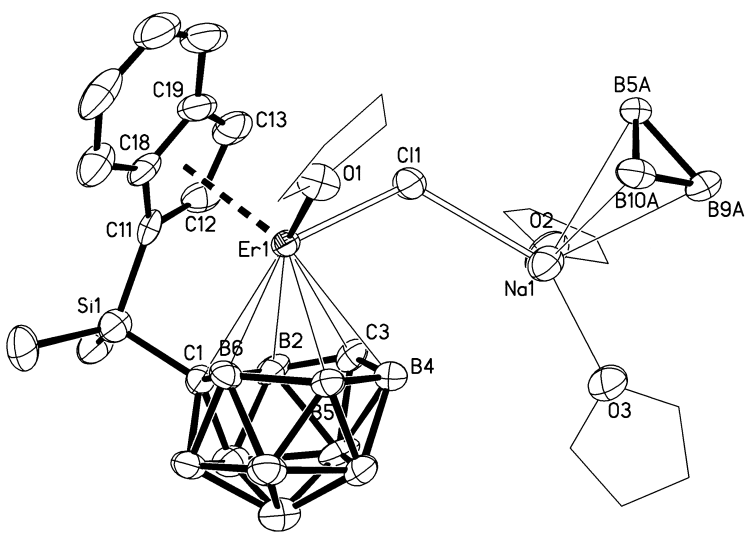

Figure 1. Molecular structure of $[\{\eta^5{:}\eta^6\text{-}Me_2Si(C_9H_6)(C_2B_{10}H_{11})\}Er(THF)(\mu\text{-}Cl)Na(THF)_2]_n$ (**2**) showing one asymmetrical unit of the infinite polymeric chain.

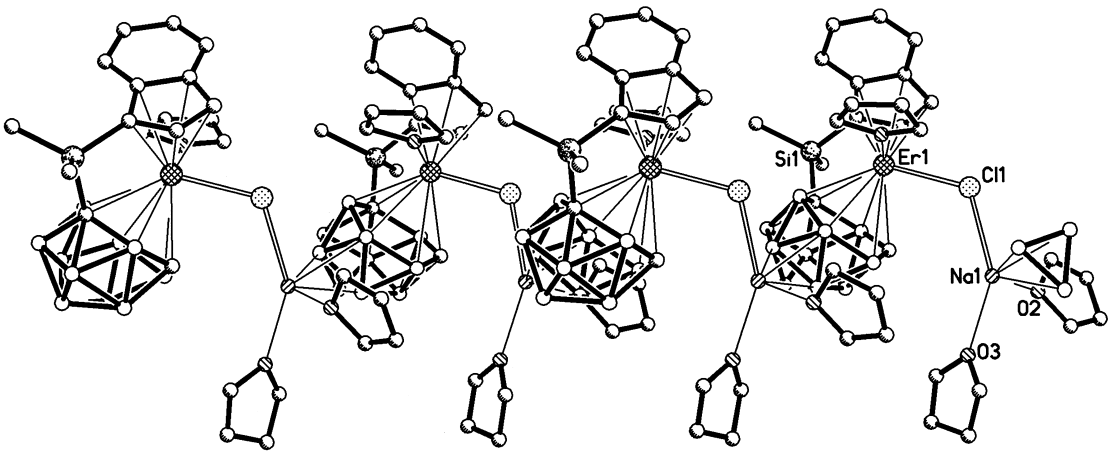

Figure 2. Perspective view of **2** revealing a portion of the infinite polymeric chain (all H atoms are omitted for clarity).

Table 1. Average bond distances (Å)

Compound	2	3	4	7	8
Ln–C(C_5 ring)	2.675(15)	2.758(5)	2.755(6)		
Ln–C(cage)	2.740(12)	2.421(5)	2.426(5)	2.360(9)	2.367(10)
Ln–B(cage)	2.790(11)	2.739(5)	2.737(7)	2.666(11)	2.644(12)
Ln···B[a]		2.921(5)	2.913(7)	2.802(11)	2.828(12)
Na···B[a]	3.017(17)	3.022(6)	3.014(7)	2.916(12)	2.900(13)

[a] Distances in M–H–B bonding.

$(C_9H_6)(C_2B_{10}H_{11})$]Ln}{$Na_2(THF)_4$} fragments that are connected through four B–H–Ln bonds. The asymmetrical units are then linked to each other via B–H–Na bonds to form an infinite polymeric chain (Fig. 4). Each Ln^{3+} ion is η^7-bound to [*arachno*-$C_2B_{10}H_{11}]^{4-}$, η^5-bound to indenyl, and σ-bound to two B–H bonds from the neighboring [*arachno*-$C_2B_{10}H_{11}]^{4-}$ unit in a distorted-tetrahedral arrangement. The geometry of the 13-vertex *closo*-metallacarborane cores is very similar to that observed in [{[η^5:η^7-$Me_2C(C_5H_4)(C_2B_{10}H_{11})$]Er}$_2${$Na_4(THF)_9$}]$_n$.[9] The Ln–C ($C_5$ ring) distances range from 2.691(5) to 2.838(5) Å in **3** and 2.691(5)–2.835(6) Å in **4**, which indicate a slip distortion of Ln toward the side of C(11)–C(12) bond. The average Ln–C(C_5 ring), Ln–C(cage) and Ln–B(cage) distances (Table 1) are all longer than the corresponding values found in its cyclopentadienyl analogue of [{[η^5:η^7-$Me_2C(C_5H_4)(C_2B_{10}H_{11})$]Er}$_2${$Na_4(THF)_9$}]$_n$.[9]

These results demonstrate the similarities and differences between the cyclopentadienyl- and indenyl–carboranyl ligands. The latter can weaken metal–ligand interactions due to steric/electronic reasons. As a result, lanthanide carborane complexes with different molecular structures were prepared.

2.2. Metallacarboranes with bis-substituted carborane ligands

2.2.1. Synthesis. To investigate the substituents effect, two other carboranes were prepared as shown in Scheme 2. It might be anticipated that the oxygen atoms of **5** and the large π system of **6** could possibly alter the interactions between the central metal ion and *arachno*-carborane ligand, resulting in a new structural motif. Both compounds were fully characterized by various spectroscopic data. Their ^{11}B NMR spectra exhibit the same 1:4 splitting pattern. The chemical shifts of methylene protons are quite different, 3.80 ppm in **5** and 4.82 ppm in **6**, respectively.

Reaction of **6** with excess finely cut Na metal in THF followed by treatment with 1 equiv. of $LnCl_3$ (Ln=Er, Y) gave a large amount of precipitates during the reaction. The resultant complexes did not dissolve in any organic solvents even dimethylformamide (DMF) and pyridine, which made

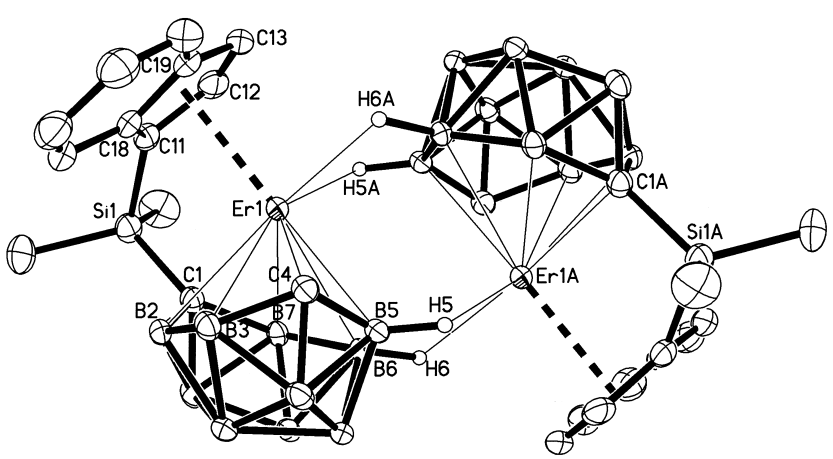

Figure 3. Molecular structure of [{η^5:η^7-$Me_2Si(C_9H_6)(C_2B_{10}H_{11})$}Er]$_2^{4-}$ in **3**.

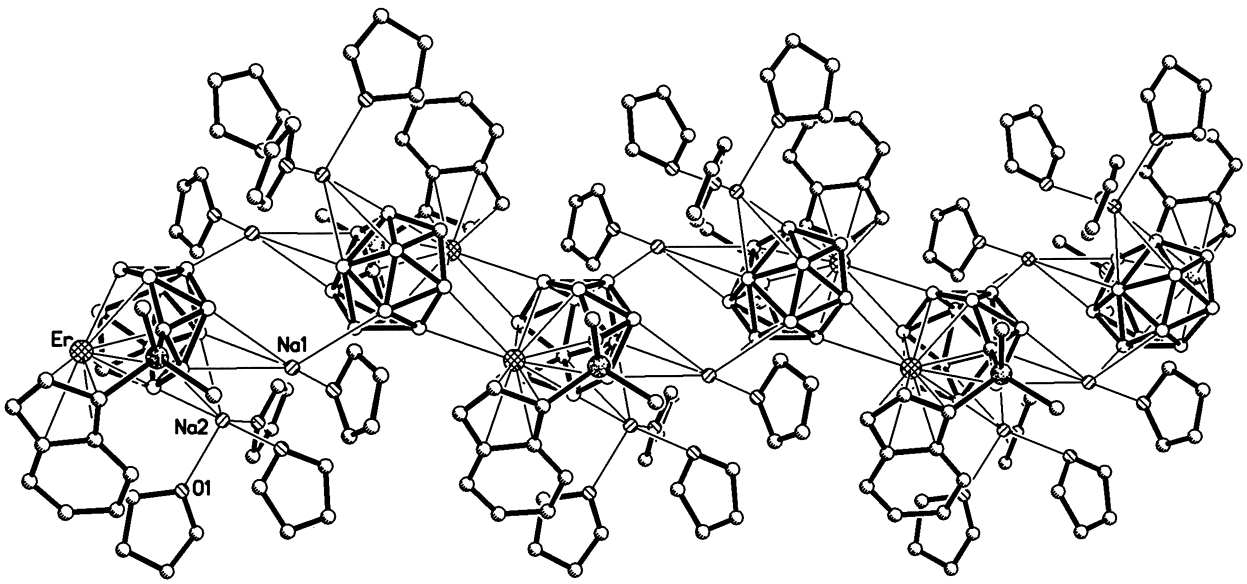

Figure 4. Perspective view of **3** revealing a portion of the infinite polymeric chain (all H atoms are omitted for clarity).

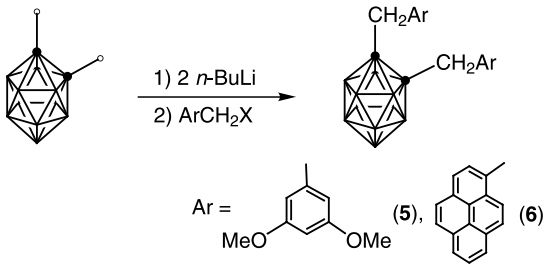

Scheme 2.

the characterization of these complexes infeasible. We then turned to compound **5**.

Interaction of **5** with excess finely cut Na metal in THF followed by treatment with 1 equiv. of $LnCl_3$ (Ln=Er, Y) gave, after recrystallization from THF, $[\{[\eta^7\text{-}(3,5\text{-}(CH_3O)_2C_6H_3CH_2)_2C_2B_{10}H_{10}]Ln(THF)\}\{Na(THF)_3\}]_2$ (Ln=Er (**7**), Y (**8**)) in moderate yields, shown in Scheme 3. They were fully characterized by various spectroscopic data and elemental analyses. The ^1H NMR spectrum of **8** supported the ratio of four THF molecules per carboranyl ligand. The two methylene groups are chemically quite different with the chemical shifts of 4.99 and 4.22 ppm, respectively. In addition, the two methylene protons are diastereotopic with the coupling constant of 12.6 Hz. Its ^{11}B NMR exhibited a 2:2:3:2:1 splitting pattern, which differs significantly from the parent carborane **5**. Thus ^{11}B NMR can serve as a useful probe to monitor this reaction.

Single-crystal X-ray analyses reveal that complexes **7** and **8** are neither isostructural nor isomorphous although their compositions are identical except for the central metals, which is not common in rare earth chemistry.[11] Their solid-state structures are shown in Figures 5 and 6, respectively. The main differences between two structures are that (1) **8** is a centrosymmetric dimer while **7** is not, and (2) the orientation of one out of three methoxy groups per carboranyl cage are different. The geometry of the *arachno*-carborane moiety and coordination sphere around rare earth atoms in two complexes are very similar. Each Ln^{3+} ion is η^7-bound to $[arachno\text{-}R_2C_2B_{10}H_{10}]^{4-}$, σ-bound to two B–H bonds from the C_2B_5 bonding face of the neighboring $[arachno\text{-}R_2C_2B_{10}H_{10}]^{4-}$ unit and coordinated to one THF in a highly distorted-tetrahedral arrangement. This structural motif is almost identical with that observed in $[\{[\eta^7\text{-}(C_6H_5CH_2)_2C_2B_{10}H_{10}]Ln(THF)\}\{Na(THF)_3\}]_2$.[6] The average Er–C(cage) and Er–B(cage) distances of 2.360(9) and 2.666(11) Å in **7** (Table 1) are almost the same as those of 2.366(2) and 2.665(2) Å found in $[\{[\eta^7\text{-}(C_6H_5CH_2)_2C_2B_{10}H_{10}]Er(THF)\}\{Na(THF)_3\}]_2$, respectively.[6] The corresponding values of 2.367(10) and 2.644(12) Å in **8** are, however, considerably shorter than the 2.392(3) and 2.689(3) Å observed in $[\{[\eta^7\text{-}(C_6H_5CH_2)_2C_2B_{10}H_{10}]Y(THF)\}\{Na(THF)_3\}]_2$, respectively.[6] The distances between two about parallel aromatic rings are ~7.07 Å in **7** and ~6.82 Å in **8**, which force the THF molecule to be coplanar with them as much as possible to minimize steric interactions (Fig. 7). There are no

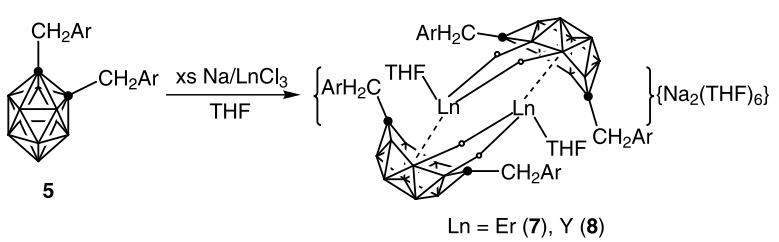

Scheme 3.

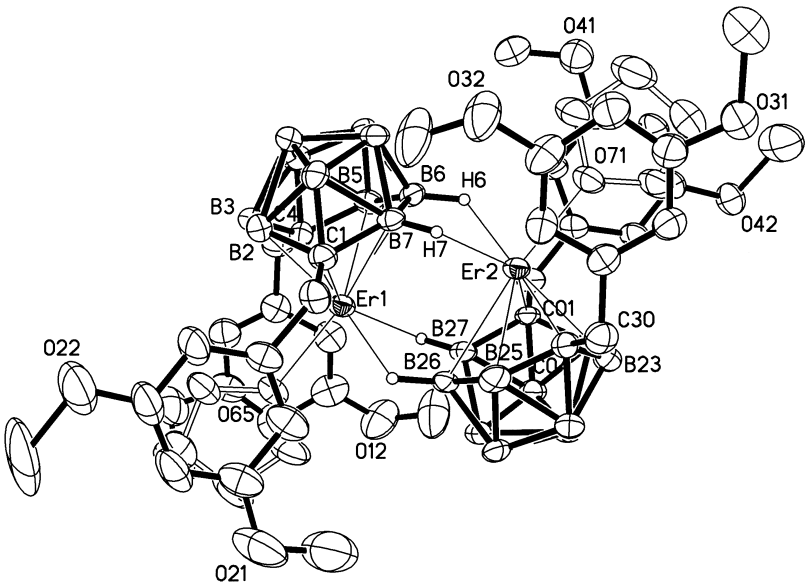

Figure 5. Molecular structure of $[\{\eta^7\text{-}(3,5\text{-}(CH_3O)_2C_6H_3CH_2)_2C_2B_{10}H_{10}\}Er(THF)]_2^{2-}$ in **7**.

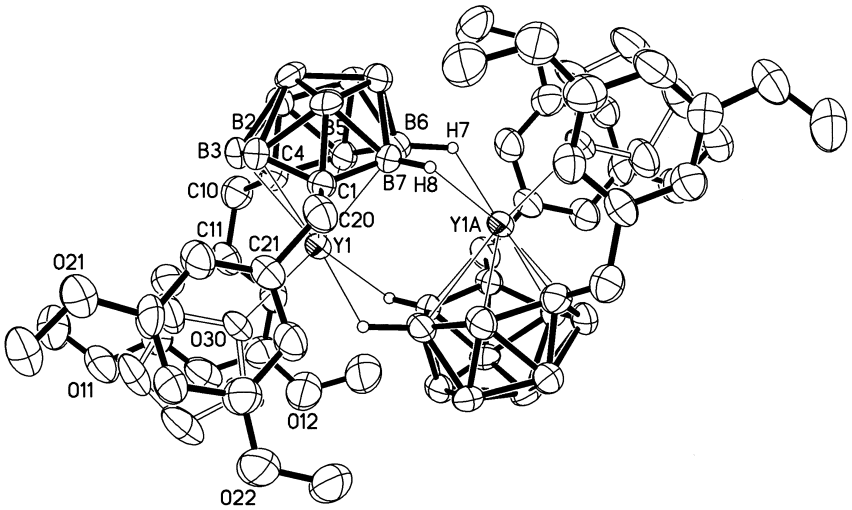

Figure 6. Molecular structure of $[\{\eta^7\text{-}(3,5\text{-}(CH_3O)_2C_6H_3CH_2)_2C_2B_{10}H_{10}\}Y(THF)]_2^{2-}$ in **8**.

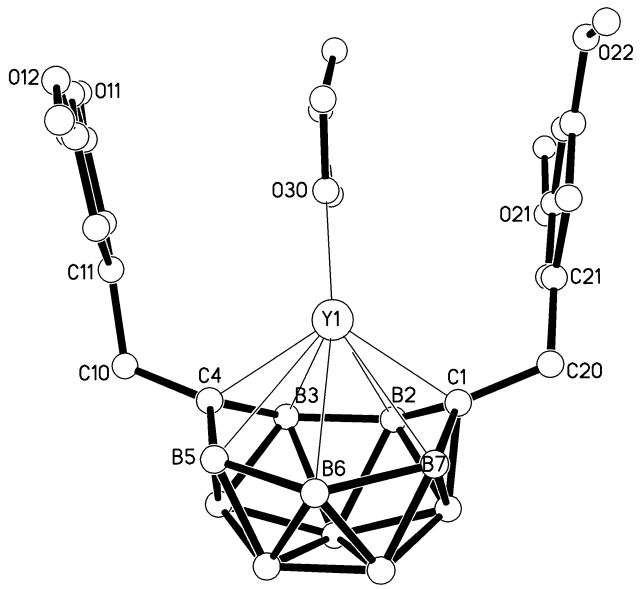

Figure 7. Closer view of the coordination environment of Y atom in **8**.

interactions between the central metal ion and any one of the methoxy groups.

This work indicates that the substituents on carborane cage carbons may affect the overall molecular structures of the 13-vertex *closo*-metallacarborane complexes, but have little influence on the interactions between the central metal ion and *arachno*-carborane ligand.

3. Experimental

3.1. General

All experiments were preformed under an atmosphere of dry dinitrogen with the rigid exclusion of air and moisture using standard Schlenk or cannula techniques, or in a glovebox. All organic solvents were freshly distilled from sodium benzophenone ketyl immediately prior to use. $Me_2Si(C_9H_7)(C_2B_{10}H_{11})$ (**1**)[8] and 1-(chloromethyl)pyrene[12] were prepared according to literature methods. All chemicals were

purchased from either Aldrich or Acros Chemical Co. and used as received. Infrared spectra were obtained from KBr pellets prepared in the glovebox on a Perkin–Elmer 1600 Fourier transform spectrometer. ^{1}H and ^{13}C NMR spectra were recorded on a Bruker DPX 300 spectrometer at 300.13 and 75.47 MHz, respectively. ^{11}B NMR spectra were recorded on a Varian Inova 400 spectrometer at 128.32 MHz. All chemical shifts are reported in δ units with references to the residual protons of the deuterated solvents for proton and carbon chemical shifts and to external $BF_3{\cdot}OEt_2$ (0.00 ppm) for boron chemical shifts. Elemental analyses were performed by MEDAC Ltd, Brunel University, Middlesex, UK.

3.1.1. Preparation of [{η^5:η^6-$Me_2Si(C_9H_6)(C_2B_{10}H_{11})$}-Er(THF)($\mu$-Cl)Na(THF)$_2$]$_n$ (2). NaH powder (0.024 g, 1.00 mmol) was added to a THF solution (15 mL) of $Me_2Si(C_9H_7)(C_2B_{10}H_{11})$ (**1**; 0.32 g, 1.00 mmol). The mixture was stirred at room temperature for 2 h. Finely cut Na metal (0.10 g, 4.35 mmol) was then added to the resulting solution ($[Me_2Si(C_9H_6)(C_2B_{10}H_{11})]Na(THF)_x$) and the mixture was stirred at room temperature overnight. The resulting $[Me_2Si(C_9H_6)(C_2B_{10}H_{11})]Na_3(THF)_x$ solution was filtered into a suspension of $ErCl_3$ (0.27 g, 1.00 mmol) in THF (15 mL) at room temperature, and the reaction mixture was stirred overnight. The color of the solution was gradually changed from colorless to orange. After removal of the precipitates, the clear orange solution was concentrated to about 3 mL. Toluene (10 mL) was added. This solution was concentrated again until a crystalline solid appeared on the wall of the Schlenk flask. This suspension was then heated until the solid dissolved. The resulting saturated solution was cooled to room temperature, affording **2** as pink crystals (0.51 g, 67%). ^{1}H NMR (pyridine-d_5): δ 64.0 (br s), 54.2 (br s), 20.8 (br s), 3.6 (m), 1.5 (m), −10.8 (br s), −40.7 (br s), −54.0 (br s), −58.6 (br s). ^{13}C NMR (pyridine-d_5): many broad, unresolved resonances. ^{11}B NMR (pyridine-d_5): δ −31.4 (1), −42.8 (2), −79.7 (2), −99.6 (2), −144.0 (1), −154.4 (2). IR (KBr, cm^{-1}): ν 3066 (m), 2977 (s), 2873 (s), 2533 (vs), 2496 (vs), 2467 (s), 2400 (s), 1450 (s), 1404 (s), 1330 (s), 1296 (s), 1247 (s), 1143 (s), 1048 (s), 1003 (s), 893 (s), 830 (s), 784 (s), 750 (s), 670 (s), 440 (s). Anal. calcd for $C_{21}H_{39}B_{10}ClErNaO_2Si$ (**2**-THF): C, 36.80; H, 5.74. Found: C, 37.12; H, 5.69.

3.1.2. Preparation of [{η^5:η^7-$[Me_2Si(C_9H_6)(C_2B_{10}H_{11})]$-Er}$_2${$Na_4(THF)_8$}]$_n$ (3). Finely cut Na metal (0.10 g, 4.35 mmol) was added to a THF (20 mL) solution of **2** (0.30 g, 0.40 mmol), and the reaction mixture was stirred at room temperature for 5 days. After removal of the precipitates, the clear orange solution was concentrated to about 2 mL. Toluene (10 mL) was added. Slow evaporation at room temperature gave **3** as pink crystals (0.22 g, 66%). Both ^{1}H and ^{13}C NMR spectra in pyridine-d_5 were unable to be recorded due to the loss of lock signals. ^{11}B NMR (pyridine-d_5): many very broad, unresolved resonances. IR (KBr, cm^{-1}): ν 3061 (m), 2956 (s), 2876 (s), 2404 (vs), 1462 (s), 1389 (m), 1325 (s), 1289 (m), 1240 (s), 1137 (s), 1047 (s), 882 (s), 829 (s), 800 (s), 763 (s), 663 (s), 559 (s), 448 (s). Anal. calcd for $C_{42}H_{78}B_{20}Er_2Na_4O_4Si_2$ (**3**–4THF): C, 37.48; H, 5.84. Found: C, 37.66; H, 5.87.

This complex was also prepared in 60% yield from reaction of $ErCl_3$ with 1 equiv. of **1** and NaH in the presence of excess Na in THF, followed by procedures similar to those described above.

3.1.3. Preparation of [{η^5:η^7-$[Me_2Si(C_9H_6)(C_2B_{10}H_{11})]$-Dy}$_2${$Na_4(THF)_8$}]$_n$ (4). NaH powder (0.024 g, 1.00 mmol) was added to a THF solution (15 mL) of $Me_2Si(C_9H_7)(C_2B_{10}H_{11})$ (**1**; 0.32 g, 1.00 mmol) and the mixture was stirred at room temperature for 2 h. Finely cut Na metal (0.13 g, 5.65 mmol) and a THF (15 mL) suspension of $DyCl_3$ (0.27 g, 1.00 mmol) were added to the resulting solution ($[Me_2Si(C_9H_6)(C_2B_{10}H_{11})]Na(THF)_x$). The reaction mixture was then stirred at room temperature for 2 days, using the procedure identical to that reported for **3** to give **4** as pale-yellow crystals (0.46 g, 57%). Both ^{1}H and ^{13}C NMR spectra in pyridine-d_5 were unable to be recorded due to the loss of lock signals. ^{11}B NMR (pyridine-d_5): many very broad, unresolved resonances. IR (KBr, cm^{-1}): ν 3058 (m), 2956 (s), 2878 (m), 2436 (vs), 2353 (vs), 2320 (s), 1603 (s), 2533 (m), 1451 (s), 1387 (s), 1326 (m), 1246 (s), 1043 (vs), 780 (s), 768 (s), 662 (s), 547 (s), 495 (m), 447 (m). Anal. calcd for $C_{26}H_{46}B_{20}Dy_2Na_4Si_2$ (**4**–8THF): C, 29.80; H, 4.42. Found: C, 29.76; H, 4.41.

3.1.4. Preparation of 1,2-[3,5-$(CH_3O)_2C_6H_3CH_2]_2$-1,2-$C_2B_{10}H_{10}$ (5). A 1.60 M solution of *n*-BuLi in *n*-hexane (12.5 mL, 20.0 mmol) was slowly added to a solution of *o*-$C_2B_{10}H_{12}$ (1.44 g, 10.0 mmol) in a dry toluene/Et_2O (2:1) mixture (18 mL) at −78°C. The mixture was allowed to warm to room temperature and stirred for 1 h. The resulting $Li_2C_2B_{10}H_{10}$ solution was then cooled to 0°C. A solution of 3,5-dimethoxybenzyl bromide (4.90 g, 21.2 mmol) in toluene/Et_2O mixture (15 mL) was added dropwise. The reaction mixture was refluxed overnight and quenched with 30 mL of water. The organic layer was separated, and the aqueous layer was extracted with Et_2O (3×15 mL). The combined organic portions were dried over anhydrous $MgSO_4$. Removal of the solvents and recrystallization from Et_2O gave **5** as a white crystalline solid (2.68 g, 60%). ^{1}H NMR ($CDCl_3$): δ 6.43 (m, 2H, aryl *H*), 6.36 (m, 4H, aryl *H*), 3.80 (s, 12H, OCH_3), 3.54 (s, 4H, CH_2). ^{13}C NMR ($CDCl_3$): δ 160.8, 136.9, 108.7, 99.6 (aryl *C*), 79.2 (cage *C*), 55.4 (OCH_3), 41.6 (CH_2). ^{11}B NMR ($CDCl_3$): δ −5.1(2), −10.7(8). IR (KBr, cm^{-1}): ν 2947 (m), 2865 (w), 2589 (vs), 2324 (w), 1603 (vs), 1455 (s), 1324 (m), 1174 (s), 1053 (s), 822(s), 693 (w). Anal. calcd for $C_{20}H_{32}B_{10}O_4$: C, 54.03; H, 7.26. Found: C, 54.00; H, 6.94.

3.1.5. Preparation of 1,2-$(C_{16}H_9CH_2)_2$-1,2-$C_2B_{10}H_{10}$ (6). A 1.60 M solution of *n*-BuLi in *n*-hexane (12.5 mL, 20.0 mmol) was slowly added to a solution of *o*-$C_2B_{10}H_{12}$ (1.44 g, 10.0 mmol) in a dry toluene/Et_2O mixture (2:1, 30 mL) at 0°C. The mixture was allowed to warm to room temperature and stirred for 30 min. The solution was then cooled to 0°C, and 1-(chloromethyl)pyrene (6.26 g, 25.0 mmol) powder was slowly added with stirring. The reaction mixture was refluxed for 3 days. After removal of most of the solvents, water (30 mL) was then added. The precipitate was collected by filtration and washed with *n*-hexane (10 mL×2). Recrystallization from THF afforded **6** as a yellow crystalline solid (2.29 g, 40%). ^{1}H NMR ($CDCl_3$): δ 8.19 (m, 18H, $C_{16}H_9CH_2$), 4.82 (s, 4H, $C_{16}H_9CH_2$). ^{13}C NMR ($CDCl_3$): δ 132.2, 131.5, 130.9,

Table 2. Crystal data and summary of data collection and refinement for **2**-**4** and **7**-**8**

	2	**3**	**4**	**7**	**8**
Formula	$C_{25}H_{47}B_{10}ClErNaO_3Si$	$C_{58}H_{110}B_{20}Er_2Na_4O_8Si_2$	$C_{58}H_{110}B_{20}Dy_2Na_4O_8Si_2$	$C_{72}H_{128}B_{20}Er_2Na_2O_{16}$	$C_{72}H_{128}B_{20}Na_2O_{16}Y_2$
Crystal size (mm)	0.30×0.30×0.25	0.48×0.34×0.32	0.50×0.25×0.25	0.56×0.45×0.25	0.63×0.45×0.16
fw	757.5	1634.3	1624.8	1846.4	1689.7
Crystal system	Orthorhombic	Triclinic	Triclinic	Monoclinic	Monoclinic
Space group	*Pbca*	*P*(-1)	*P*(-1)	$P2_1/n$	$P2_1/n$
a (Å)	12.857(2)	12.099(1)	12.078(1)	16.407(1)	12.172(2)
b (Å)	13.219(4)	13.335(1)	13.313(1)	25.362(2)	16.109(3)
c (Å)	41.609(5)	14.760(1)	14.750(1)	21.777(2)	22.924(5)
α (°)	90	115.08(1)	115.10(1)	90	90
β (°)	90	91.16(1)	91.17(1)	90.25(1)	97.02(3)
γ (°)	90	115.13(1)	115.17(1)	90	90
V (Å^3)	7072(3)	1893.3(2)	1884.5(2)	9061(1)	4461(2)
Z	8	1	1	4	2
D_{calcd} (mg/m^3)	1.423	1.433	1.432	1.353	1.258
Radiation (λ) (Å)	Mo Kα (0.71073)	Mo Kα (0.71073)	Mo Kα (0.71073)	Mo Kα (0.71073)	Mo Kα (0.71073)
2θ range (°)	3.7–50.0	3.2–56.0	3.2–50.0	2.4–50.0	4.2–50.0
μ (mm^{-1})	2.521	2.303	2.070	1.907	1.363
F(000)	3048	830	826	3784	1776
No. of obsd reflns	6186	8944	6601	15959	7843
No. of params refnd	381	464	464	959	545
Goodness-of-fit	1.081	1.019	0.846	0.987	0.909
*R*1	0.067	0.046	0.040	0.063	0.074
*WR*2	0.105	0.104	0.098	0.161	0.173

130.0, 129.0, 128.5, 127.7, 126.6, 126.3, 126.0, 125.3, 124.9, 123.1 ($C_{16}H_9CH_2$), 40.6 ($C_{16}H_9CH_2$). ^{11}B NMR ($CDCl_3$): δ −4.3 (2B), −10.7 (8B). IR (KBr, cm^{-1}): ν 3039 (w), 2585 (vs), 1595 (m), 1180 (m), 1074 (m), 1012 (m), 841 (vs), 704 (m). MS (FAB): 574 with correct isotope distribution.

3.1.6. Preparation of [{[η^7-(3,5-$(CH_3O)_2C_6H_3CH_2)_2C_2B_{10}H_{10}$]Er(THF)}{Na(THF)$_3$}]$_2$ (7). Finely cut Na metal (0.11 mg, 4.78 mmol) was added to a THF solution (20 mL) of 1,2-[3,5-$(CH_3O)_2C_6H_3CH_2]_2$-1,2-$C_2B_{10}H_{10}$ (**5**; 0.21 mg, 0.47 mmol) at room temperature, and the mixture was stirred overnight. $ErCl_3$ (0.13 mg, 0.47 mmol) was added to the resulting solution, and the reaction mixture was stirred at room temperature for 4 days. After removal of the precipitates, the resulting clear THF solution was concentrated under vacuum to about 5 mL from which **7** was isolated as pink crystals after this solution stood at room temperature for several days (0.25 g, 58%). ^{1}H NMR (pyridine-d_5): δ 8.25 (d, *J*=9.0 Hz), 7.33 (m), 7.01 (m), 6.96 (d, *J*=3.9 Hz), 6.25 (d, *J*=3.6 Hz), 6.18 (d, *J*=8.4 Hz), 3.63 (m), 1.61 (m), 3.39 (s), 2.56 (s), 2.37 (s), 1.97 (s), 1.76 (s). ^{13}C NMR (pyridine-d_5): δ 138.6, 126.0, 125.6, 125.1, 124.6, 123.7, 119.7, 99.2, 67.2, 47.0, 44.7, 35.6, 33.4, 32.5, 25.1. ^{11}B NMR (pyridine-d_5): δ −4.5 (2), −5.9 (2), −9.9 (6). IR (KBr, cm^{-1}): ν 2956 (m), 2888 (m), 2462 (vs), 1598 (vs), 1459 (s), 1320 (w), 1199 (m), 1150 (vs), 1054 (vs), 808 (m), 696 (w). Anal. calcd for $C_{72}H_{128}B_{20}Er_2Na_2O_{16}$: C, 46.83; H, 6.99. Found: C, 46.94; H, 6.81.

3.1.7. Preparation of [{[η^7-(3,5-$(CH_3O)_2C_6H_3CH_2)_2C_2B_{10}H_{10}$]Y(THF)}{Na(THF)$_3$}]$_2$ (8). This complex was prepared as pale-yellow crystals from YCl_3 (0.09 g, 0.46 mmol), **5** (0.21 g, 0.47 mmol), and Na metal (0.11 g, 4.78 mmol) in 20 mL of THF using the procedure, identical to that reported for **7**: yield 0.19 g (49%). ^{1}H NMR (pyridine-d_5): δ 7.07 (s, 4H, *o*-aryl *H*), 5.97 (s, 2H, *p*-aryl *H*), 4.99 (d, *J*=12.6 Hz, 2H, CH_2), 4.22 (d, *J*=12.6 Hz, 2H, CH_2), 3.75 (s, 12H, OCH_3), 3.64 (m, 16H, THF), 1.62 (m, 16H, THF). ^{13}C NMR (pyridine-d_5): δ 159.7, 150.2, 106.9, 98.5 (aryl *C*), 67.2, 25.2 (THF), 54.5 (OCH_3), 52.4 (CH_2). ^{11}B NMR (pyridine-d_5): δ 1.2 (2), −15.8 (2), −19.6 (3), −25.0 (2), −36.3 (1). IR (KBr, cm^{-1}): ν 2953 (m), 2517 (m), 2352 (vs), 1599 (vs), 1459 (s), 1325 (m), 1199 (s), 1150 (vs), 1056 (s), 831 (w), 676 (m). Anal. calcd for $C_{72}H_{128}B_{20}Na_2O_{16}Y_2$: C, 51.18; H, 7.64. Found: C, 50.85; H, 7.63.

3.2. X-Ray structure determination

All single crystals were immersed in Paraton-N oil and sealed under N_2 in thin-walled glass capillaries. Data were collected at 293 K on a Bruker SMART 1000 CCD diffractometer using Mo Kα radiation. An empirical absorption correction was applied using the SADABS program.[13] All structures were solved by direct methods and subsequent Fourier difference techniques and refined anisotropically for all non-hydrogen atoms by full-matrix least squares calculations on F^2 using the SHELXTL program package.[14] Most of the carborane hydrogen atoms were located from difference Fourier syntheses. All other hydrogen atoms were geometrically fixed using the riding model. Crystal data and details of data collection and structure refinements are given in Table 2. Crystallographic data (excluding structure factors) for the structures in this paper have been deposited with the Cambridge Crystallographic Data Centre as supplementary publication numbers CCDC-207613 to CCDC-207617 for **2**-**4**, **7** and **8**, respectively. Copies of the data can be obtained, free of charge, on application to CCDC, 12 Union Road, Cambridge, CB2 1EZ, UK.

Acknowledgements

The work described in this paper was supported by a grant

from the Research Grants Council of the Hong Kong Special Administration Region (Project No. CUHK 4254/01P).

References

1. (a) Grimes, R. N. *Comprehensive Organometallic Chemistry II*; Abel, E. W., Stone, F. G. A., Wilkinson, G., Eds.; Pergamon: New York, 1995; Vol. 1, p 373. (b) Grimes, R. N. *Coord. Chem. Rev.* **2000**, *200/202*, 773.
2. (a) Saxena, A. K.; Hosmane, N. S. *Chem. Rev.* **1993**, *93*, 1081. (b) Saxena, A. K.; Maguire, J. A.; Hosmane, N. S. *Chem. Rev.* **1997**, *97*, 2421.
3. (a) Xie, Z. *Coord. Chem. Rev.* **2002**, *231*, 23. (b) Xie, Z. *Pure Appl. Chem.* **2001**, *73*, 361.
4. Xie, Z. *Acc. Chem. Res.* **2003**, *36*, 1.
5. Xie, Z.; Yan, C.; Yang, Q.; Mak, T. C. M. *Angew. Chem., Int. Ed.* **1999**, *38*, 1761.
6. Chui, K.; Yang, Q.; Mak, T. C. W.; Lam, W.-H.; Lin, Z.; Xie, Z. *J. Am. Chem. Soc.* **2000**, *122*, 5758.
7. O'Connor, J. M.; Casey, C. P. *Chem. Rev.* **1987**, *87*, 307.
8. Xie, Z.; Wang, S.; Yang, Q.; Mak, T. C. W. *Organometallics* **1999**, *18*, 2420.
9. Chui, K.; Yang, Q.; Mak, T. C. W.; Xie, Z. *Organometallics* **2000**, *19*, 1391.
10. Wang, S.; Yang, Q.; Mak, T. C. W.; Xie, Z. *Organometallics* **1999**, *18*, 4478.
11. Schumann, H.; Messe-Markscheffel, J. A.; Esser, L. *Chem. Rev.* **1995**, *95*, 865.
12. Bair, K. W.; Tuttle, R. L.; Knick, V. C.; Cory, M.; Mckee, D. D. *J. Med. Chem.* **1990**, *33*, 2385.
13. Sheldrick, G. M., *SADABS*: *Program for Empirical Absorption Correction of Area Detector Data*; University of Göttingen: Germany, 1996.
14. Sheldrick, G. M. *SHELXTL 5.10 for windows NT*: *Structure Determination Software Programs*; Bruker Analytical X-ray systems, Inc.: Madison, Wisconsin, USA, 1997.